Chinese Journal of Aeronautics, (2020), 33(4): 1288–1298

Chinese Society of Aeronautics and Astronautics
& Beihang University

Chinese Journal of Aeronautics

cja@buaa.edu.cn
www.sciencedirect.com

An energy-based coupling degradation propagation model and its application to aviation actuation system

Tongyang LI [a,b], **Shaoping WANG** [a], **Jian SHI** [a,*], **Enrico ZIO** [b,c,d], **Xiaoyu CUI** [a]

[a] *School of Automation Science and Electrical Engineering, Beihang University, Beijing 100083, China*
[b] *Energy Department, Politecnico di Milano, Via La Masa 34, Milano 20156 , Italy*
[c] *MINES ParisTech, PSL Research University, CRC, Sophia Antipolis, 06410, France*
[d] *Department of Nuclear Engineering, College of Engineering, Kyung Hee University, Gyeonggi-do 12001, South Korea*

Received 7 May 2019; revised 25 July 2019; accepted 7 September 2019
Available online 12 February 2020

KEYWORDS

Actuation system;
Cascading failure;
Complex system;
Failure propagation;
Mechatronic system

Abstract The degradation of components in complex mechatronic systems involves multiple physical processes which will cause coupling interactions among nodes in the system. The interaction of nodes may be carried out not only by physical connections but also by the environment which cannot be described by single network using the traditional methods. In order to give out a unified model to quantitatively describe the coupling degradation spreading by both physical connections and environment, a novel Energy-Flow-Field Network (EFFN) and a coupling degradation model based on EFFN are proposed in this paper. The EFFN is driven by energy flow and the state transition of spatially related nodes is triggered by the dissipation energy. An application is conducted on aviation actuation system in which the degradation spreading by fluid-thermal-solid interaction is considered. The degradation path and the most probable fault reason can be obtained by combining the state transition and energy output of nodes, which is consistent with the given scenario.

1. Introduction

Systems such as production system in modern process industry, power supplying system of a high-speed train[1] and actuation system in an aircraft[2] are complex mechatronic systems which involve multiple physical processes including mechanics, electrics and hydro-mechanics. With growing complexity, an increasing interaction among components inevitably brings about threat of cascading failures in mechatronic systems, which has become a key focus currently.[3–6]

* Corresponding author.
E-mail address: shijian@buaa.edu.cn (J. SHI).

Peer review under responsibility of Editorial Committee of CJA.

https://doi.org/10.1016/j.cja.2019.11.012

Taking the topological perspective, the complex connecting relation of mechatronic components can be described as complex networks. The most famous complex networks are small world network and scale-free network. Watts and Strogatz proposed the small world network in which the connection topology is neither completely regular nor completely random.[7] Based on the small world network, Gao et al.[8] studied the fault propagation of a production system. Barabasi and Albert proposed the scale-free network[9] in which new nodes can be added into the network and attached to the nodes which are already well connected. The two networks solved the increasing topological complexity by extending networks with arbitrary connections and scales.

The cascading failure ordinarily starts from the malfunction of a single component caused by a random trigger, which propagates along spreading paths and finally results in a catastrophic impact on the holistic system. Overload may occur on both nodes and edges and is believed as the main causes in many real cases. Ren et al.[10] focused on the effect of load distribution law on the power grid which is regarded as a complex network with generators, substations and consumers. Wei et al.[11] analyzed the cascading failure faults in transmission networks combining complex network theory with cascading faults graphs. Jing and Tang[12] evaluated the effect of cascading failure considering the characteristics of time delay and recovery strategy. Lin et al.[13,14] assessed the reliability of complex electromechanical system using complex network method. There are also research studies concerning the cascading overload failures caused by network load dynamics. Zhang et al.[15] established a probabilistic cascade failure model using mean field theory and impact of initial load and tolerance parameter distribution on cascade failure was investigated. Zhang and Yağan[16] analyzed the load dynamic in electrical power systems and the robustness was optimized.

It has been identified that cascading failures in real-world systems are also caused by interdependency among components. There are various failure modes for different mechatronic components, i.e., failure modes of an aviation hydraulic pump involve bearing failure, internal friction wear, piston head gap increase and swash plate incline[17,18]. Most of the failure modes are not independent like the internal friction wear which may also be intensified by higher working pressure caused by other components in the system. Liu et al.[19] utilized the node-coupling strength to describe the dependency between nodes and the percolation framework was used to study the robustness of the networks. There are also research studies concerning the interdependency among different networks. Based on percolation theory, Su et al.[20] analyzed cascading failures on interdependent networks using multiple dependency links and cliques. Zhong et al.[21] investigated the restoration of interdependent network after cascading overload failure using a load-dependent cascading model. Liu et al.[22] studied the percolation in coupled networks considering both inner-dependency and inter-dependency.

The relation of components in mechatronic systems is jointly affected by load dynamics and dependency among components. Probably, in an aviation actuation system, an accident starts from a initially slight fault on a component like an actuator clamping, and then, the motor connected to the actuator is blocked and generates more heat which rises the operating temperature and finally leads to a systematic failure.[2] In this scenario, failure spreads from actuator to motor by physical links, from motor to other part of the system by environment. Similar impacts of environment may be carried out by vibrations and electromagnetic fields.[23] These complicated spreading paths display a cumulative characteristic and attenuate with spatial distance of the components.[24] In this paper, overload on a single component is believed to be the start point in a cascading failure, while the block of a motor may not cause a shock failure, but a gradual degradation instead, which means that the influence on the other components in mechatronic system begins when the working condition changes.

Based on the aforementioned methods, the overload spreading along physical connections and the influence spreading by environment can be regarded as two interdependent networks. Since the interaction of multiple physical processes is complex in mechatronic systems, it is difficult to define the load-dependent relation between the two networks. Aimed at giving out a unified model to quantitatively describe the coupling degradation spreading by both physical connections and environment, this paper proposes a universal Energy-Flow-Field Network (EFFN). In EFFN, components are nodes with energy capacities and spatial structure linked by edges with strength and length. Changing the state of a node will conduct a physical impact on the connected nodes and an accumulative field impact on the nodes closed in space dimension, which means that degradation propagates along both physical links and temperature or electromagnetic field. A certain capacity degradation of a node according to the degradation mode and its corresponding severe degree will have a coupling effect on the related nodes which is described as a coupling degradation coefficient matrix in this work. The propagation paths solving of the proposed network follows the framework of stochastic flow network[25–28] by using the concept of minimal paths and minimal cuts.

The rest of the paper is organized as follows: in Section 2, the problem is described in detail and some basic assumptions are proposed. Section 3 introduces the novel EFFN and the degradation propagation and coupling model based on the network. In Section 4, the application of the model to an aviation actuation system is presented. Conclusions are drawn in Section 5.

2. Problem description and assumptions

In traditional networks, when the load on a node exceeds its capacity, the node fails. The load is the measurement of the flow and the flow can only be transferred by edges, which reflects most normal working operation of complex systems. When degradation occurs, nodes connected to the degraded node may be also influenced and perform a lower working efficiency such as a higher congestion rate of a connected traffic intersection, a higher delay rate of a connected information point, a lower operating voltage of a connected substation and a lower working pressure of a connected pump. The degradation of nodes can be described by multistate models like stochastic flow network. For a mechatronic system, energy works as the medium flowing with different forms and the devices work as nodes transforming and transferring energy in the network. During the transforming and transferring process, it also generates heating and vibration which are triggers of degradation of other components. The influence between

two components without physical connection is recognized as field effects in this paper, and meanwhile the influence of a connected component is the flow effect.

In terms of energy, the components, devices and subsystems which are regarded as nodes in a network are points with input and output energy which converse energy among different types or transfer energy under some rules. The connections are the paths for energy transferring. Generally, energy exists in different types. In this paper, the kinetic energy, internal energy and electrical energy which flow on physical connections are named flow energy, and meanwhile, the informational energy, thermal energy, luminous energy and magnetic energy which mainly spread by the environment or other systems are regarded as field energy. Note that the definition is not unmitigated but should be determined by the actual transferring paths in a certain network. Differentiating from flow energy, field energy usually has an accumulative effect on the components in the environment. The amount of field energy on a certain component may be small but a continuous degradation threat grows with the rising of field intensity. For definiteness and without loss of generality, the original flow is redefined as the physical transfer path of energy. According to the conservation of energy, in mechatronic systems, energy will never disappear but transfer among components and environment. The proposed energy-flow-field system is assumed to satisfy the following assumptions:

(1) Energy transfer from one component to another by flow and field.
(2) Every component obeys the law of conservation of energy, while the input energy transferred by field is very small compared to the energy transferred by flow which can be neglected but can be regarded as the trigger of influence.
(3) The field energy dissipates into the local environment or other systems and gradually permeates into global environment or other systems.

3. Modeling of degradation propagation and coupling

3.1. Energy-flow-field network (EFFN)

EFFN is described by nodes and edges. Each network has only one source node. As is shown in Fig. 1, a generic node receives energy $\varphi^{(\mathrm{in})}(t)$ by flow and gives out energy $\varphi^{(\mathrm{out})}(t)$. Meanwhile, a part of energy $\psi^{(\mathrm{out})}(t)$ is dissipated in forms of field energy from the node. Energy $\psi^{(\mathrm{in})}(t)$ dissipated from other nodes are transferred by field edges into the node. Solid lines are the paths for flow and dashed lines are the paths for field. $c(t)$ stands for the capacity of the node and $c(0)$ is the rated capacity. w is the inherent energy loss consumed by the node itself and $\eta(t)$ is the efficiency of the node defined by

$$\eta(t) = \frac{w}{w + \psi^{(\mathrm{out})}(t)} \tag{1}$$

$\eta(0)$ is the rated efficiency. According to the conservation of energy,

$$\varphi^{(\mathrm{in})}(t) = \varphi^{(\mathrm{out})}(t) + \psi^{(\mathrm{out})}(t) + w \tag{2}$$

A source node generates energy $\varphi^{(\mathrm{out})}_{\mathrm{initial}}(t)$ and does not influence other nodes or is not influenced by the field. For a sink node, energy $\varphi^{(\mathrm{out})}_{\mathrm{t}}(t)$ is consumed by the node itself, and meanwhile the node may still influence other nodes and the lowest required energy of node is $w_{\mathrm{t}}(0)$. The energy balance can be described as

$$\varphi^{(\mathrm{in})}_{\mathrm{t}}(t) = \varphi^{(\mathrm{out})}_{\mathrm{t}}(t) + \psi^{(\mathrm{out})}_{\mathrm{t}}(t) + w_{\mathrm{t}}(t) \tag{3}$$

$$\eta_{\mathrm{t}}(t) = \frac{w_{\mathrm{t}}(t)}{w_{\mathrm{t}}(t) + \psi^{(\mathrm{out})}_{\mathrm{t}}(t)} \tag{4}$$

$$w_{\mathrm{t}}(t) = \varphi^{(\mathrm{out})}_{\mathrm{t}}(t) \tag{5}$$

where $e^{(\mathrm{l})}_{i,j}$ is the edge of flow energy connecting node i and node j and $P^{(\mathrm{l})}_{i,j}(l^{(\mathrm{l})}_{i,j}, s^{(\mathrm{l})}_{i,j}, d^{(\mathrm{l})}_{i,j}(t))$ is used to represent the property of this kind of edge in which $l^{(\mathrm{l})}_{i,j}$ is the length of the edge corresponding to the physical connection length, $s^{(\mathrm{l})}_{i,j} \in \{0,1\}$ is the connection strength which is defined as the probability of performing its own function in a given time or in an event and $d^{(\mathrm{l})}_{i,j}(t)$ is the energy dissipation rate per unit length. $e^{(\mathrm{i})}_{i,j}$ is the edge of field energy connecting node i and node j and its property is $P^{(\mathrm{i})}_{i,j}(s^{(\mathrm{i})}_{i,j})$ where $s^{(\mathrm{i})}_{i,j} \in \{0,1\}$ is the connection strength of the edge. For a certain edge of flow energy $\mathrm{e}^{(\mathrm{l})}_{i,j}$, $\varphi^{(\mathrm{l-in})}(t)$ is the input energy and $\varphi^{(\mathrm{l-out})}(t)$ is the output energy, as is shown in Fig. 2(a), which satisfy

$$\varphi^{(\mathrm{l-in})}_{i,j}(t) = l^{(\mathrm{l})}_{i,j} d^{(\mathrm{l})}_{i,j}(t) + \varphi^{(\mathrm{l-out})}_{i,j}(t), s^{(\mathrm{l})}_{i,j} = 1 \tag{6}$$

$$\varphi^{(\mathrm{l-out})}_{i,j}(t) = 0,\ s^{(\mathrm{l})}_{i,j} = 0 \tag{7}$$

For a field edge $e^{(\mathrm{i})}_{i,j}$, as is shown in Fig. 2(b) $\psi^{(\mathrm{i-in})}_{i,j}(t)$ is the input energy, $\psi^{(\mathrm{i-out})}_{i,j}(t)$ is the output energy and

$$\psi^{(\mathrm{i-in})}_{i,j}(t) = \psi^{(\mathrm{i-out})}_{i,j}(t), s^{(\mathrm{i})}_{i,j} = 1 \tag{8}$$

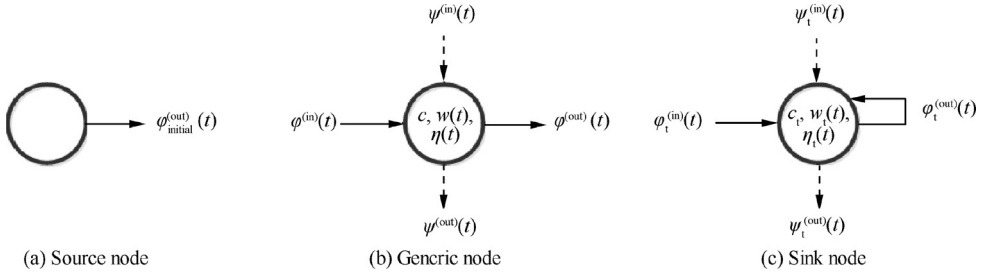

Fig. 1 Node models in EFFN.

(a) Arc of flow (b) Arc of field

Fig. 2 Edge models in EFFN.

$$\psi_{i,j}^{(\mathrm{i-out})}(t)=0, s_{i,j}^{(\mathrm{i})}=0 \tag{9}$$

Suppose that $G(\boldsymbol{V},\boldsymbol{E}^{(\mathrm{l})},\boldsymbol{E}^{(\mathrm{i})})$ describes the topology of the network, and the available paths between the source node and the sink node can then be obtained. To describe the spatial relationship of components, a Cartesian coordinate can be established. Since the absolute location of a component in the Cartesian coordinate does not influence the relative Euclidean distance of nodes, the Cartesian coordinate can be set arbitrarily. Once the coordinate system is deterministic, each node i in the coordinates system has definite location $l_i(x_i,y_i,z_i)$. If there are n nodes, $m^{(\mathrm{l})}$ edges of flow energy and $m^{(\mathrm{i})}$ edges of field energy in the network, then, $\boldsymbol{V}=[v_1,v_2,...,v_n]$ is the set of nodes, $\boldsymbol{E}^{(\mathrm{l})}=\{e_{i,j}^{(\mathrm{l})}\},\ i,j\in n$ is the set of edges of flow energy and $\boldsymbol{E}^{(\mathrm{i})}=\{e_{i,j}^{(\mathrm{i})}\},\ i,j\in n$ is the set of edges of field energy. The connections of flow edges and field edges are represented by matrix $\boldsymbol{A}^{(\mathrm{l})}$ and $\boldsymbol{A}^{(\mathrm{i})}$, respectively.

$$A^{(\mathrm{l})}=\begin{bmatrix} a_{1,1}^{(\mathrm{l})} & a_{1,2}^{(\mathrm{l})} & \cdots & a_{1,n}^{(\mathrm{l})} \\ a_{2,1}^{(\mathrm{l})} & a_{2,2}^{(\mathrm{l})} & \cdots & a_{2,n}^{(\mathrm{l})} \\ \vdots & \vdots & \ddots & \vdots \\ a_{n,1}^{(\mathrm{l})} & a_{n,2}^{(\mathrm{l})} & \cdots & a_{n,n}^{(\mathrm{l})} \end{bmatrix},$$

$$a_{i,j}^{(\mathrm{l})}=\begin{cases} 1 & \text{there is a flow connection from } \mathrm{v}_i \text{ to } v_j \text{ and } i\neq j, \\ 0 & \text{otherwise} \end{cases} \quad i,j\in n \tag{10}$$

$$A^{(\mathrm{i})}=\begin{bmatrix} a_{1,1}^{(\mathrm{i})} & a_{1,2}^{(\mathrm{i})} & \cdots & a_{1,n}^{(\mathrm{i})} \\ a_{2,1}^{(\mathrm{i})} & a_{2,2}^{(\mathrm{i})} & \cdots & a_{2,n}^{(\mathrm{i})} \\ \vdots & \vdots & \ddots & \vdots \\ a_{n,1}^{(\mathrm{i})} & a_{n,2}^{(\mathrm{i})} & \cdots & a_{n,n}^{(\mathrm{i})} \end{bmatrix},$$

$$a_{i,j}^{(\mathrm{i})}=\begin{cases} l_{i,j} & \text{there is a field connection from } \mathrm{v}_i \text{ to } v_j, \\ 0 & \text{otherwise} \end{cases} \quad i,j\in n \tag{11}$$

where $l_{i,j}=\sqrt{(x_i-x_j)^2+(y_i-y_j)^2+(z_i-z_j)^2}$. Obviously, the Euclidean distance of two connected nodes which is also the value of $l_{i,j}$ is irrelevant to the coordinate system and reference plane. Note that $\boldsymbol{A}^{(\mathrm{l})}$ is also used to identify the three types of nodes. If node i is a source node, $a_{j,i}^{(\mathrm{l})}=0,\ \forall j\in n$. If node i is a sink node, $a_{i,j}^{(\mathrm{l})}=0,\forall j\in n$. Otherwise, node i is a generic node. For the entire network, the energy balance is

$$\varphi_i^{(\mathrm{in})}(t)=\sum_{j=1}^{n-1}(w_j(t)/\eta(t))+\sum_{j=1}^{n}\sum_{k=1}^{n}l_{j,k}^{(\mathrm{l})}d_{j,k}^{(\mathrm{l})}(t) \tag{12}$$

where $\varphi_i^{(\mathrm{in})}(t)$ is the total input of the network, $\sum_{j=1}^{n-1}(w_j(t)/\eta(t))$ is the self-work and dissipation of nodes excluding the source node and $\sum_{j=1}^{n}\sum_{k=1}^{n}l_{j,k}^{(\mathrm{l})}d_{j,k}^{(\mathrm{l})}(t)$ is the transmission consumption.

Fig. 3(a) shows an aircraft actuation system. Each component of the system is a single node and the network is shown in Fig. 3(b) in which engine serves as a source node and control surface is a sink node. The spatial structure of the network follows the real location on the aircraft which is not shown in Fig. 3(a). From Fig. 3(b), we can see that the effect of pump's vibration and the effect of motor's heating on the related components are shown by field links.

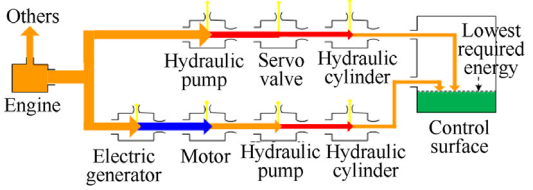

(a) Structure of a dissimilar redundancy actuation system

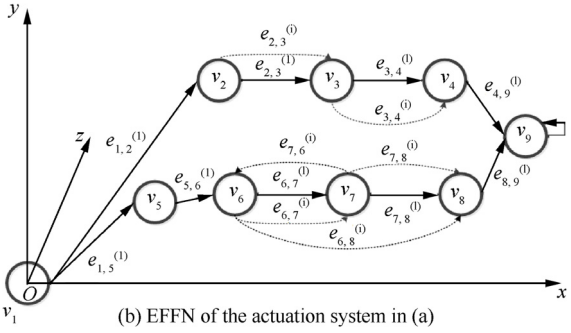

(b) EFFN of the actuation system in (a)

Fig. 3 Structure of a dissimilar redundancy actuation system.

3.2. Degradation propagation and coupling model

To study the degradation propagation, the foundation is to define the degradation and its extreme situation: failure. In the proposed EFFN, excluding source node, both nodes and edges are not perfectly reliable. An unreliable node v_i in a EFFN has the properties including capacity $c_i(t)$, self-working consumption w_i and efficiency $\eta_i(t)$. Note that for a node whose major function is to transfer energy, the inherent energy loss w_i may be at a very low level like a router or a shuttle valve, and for an energy transformation node, w_i may be at a higher level like a pump, a transformer and a motor. The irreversible part of the energy is $Ex_i(t)=w_i+\varphi_i^{(\mathrm{out})}(t)$ which

is also named as exergy in thermodynamics. The first law efficiency is defined as

$$\eta_i^{\mathrm{I}}(t) = \frac{\varphi_i^{(\mathrm{out})}(t)}{\varphi_i^{(\mathrm{in})}(t)} = \frac{\varphi_i^{(\mathrm{out})}(t)}{\varphi_i^{(\mathrm{out})}(t) + \psi_i^{(\mathrm{out})}(t) + w_i} \tag{13}$$

and the second law efficiency is given by

$$\eta_i^{\mathrm{II}}(t) = \frac{\varphi_i^{(\mathrm{out})}(t)}{Ex_i(t)} = \frac{\varphi_i^{(\mathrm{out})}(t)}{\varphi_i^{(\mathrm{out})}(t) + w_i} \tag{14}$$

Using the concept of thermodynamics, the efficiency $\eta_i(t)$ is

$$\eta_i(t) = \frac{\eta_i^{\mathrm{II}}(t)}{\eta_i^{\mathrm{I}}(t) - 2\eta_i^{\mathrm{II}}(t) + \eta_i^{\mathrm{I}}(t)\eta_i^{\mathrm{II}}(t)} \tag{15}$$

Under normal working conditions, the energy input of the node $\varphi_i^{(\mathrm{in})}(t)$ satisfies $\varphi_i^{(\mathrm{in})}(t) \geqslant w_i$. If $\varphi_i^{(\mathrm{in})}(t) < w_i$, the node stops working and $\varphi_i^{(\mathrm{out})}(t) = \psi_i^{(\mathrm{out})}(t) = 0$.The capacity limits the maximum input of the node. If $\varphi_i^{(\mathrm{in})}(t) > c_i(t)$, an overload happens, and the excess part will be added on $\psi_i^{(\mathrm{out})}(t)$ and may lead to a degradation. When degradation occurs, components in real-world systems perform a lower efficiency, while in most controlled systems, with the effect of controller, the output energy of the component remains unchanged, but the efficiency is lower than before, which means that there is larger energy input. On the other hand, the capacity of the node usually decreases corresponding to the fact that a pump leakage increases after wear. If $\boldsymbol{S}_i(t)$ is the state of node v_i at time t,

$$\boldsymbol{S}_i(t) = [c_i(t), \eta_i(t)] \tag{16}$$

If any element of $\boldsymbol{S}_i(t)$ equals zero, the node fails, otherwise, the node is normal or at a degradation stage. According to the definition of efficiency, $\eta_i(t)$ will never be zero because w_i is assumed as a constant in the proposed network. The state equals zero only when the capacity equals zero. The decrease of $\eta_i(t)$ is the reason of autologous degradation. Because this paper only focuses on the correlation of nodes, the autologous degradation model of a given component like Weibull model or an exponential model will not be discussed. Without loss of generality, the degradation state of the node is divided into slight fault, severe fault and failure, and the statement is shown in Table 1. The Autologous Degradation Rate (ADR) among the states is given in a statistical form: If N is the total number of samples, $N_{i,j}, i,j \in \{0,1,2,3\}$ is the number of samples whose states change from $S^i, i \in \{0,1,2,3\}$ to $S^j, j \in \{0,1,2,3\}$ under the efficiency $\eta(t)$ and the state changing probability $S^{i,j}$ is

Table 1 Degradation state of nodes.

Level	Description	Symbol	Capacity
Normal	The given node provides 100% output capability	S^0	$c(0)$
Slight fault	The given node provides 70% output capability	S^1	$0.7c(0)$
Severe fault	The given node provides 30% output capability	S^2	$0.3c(0)$
Failure	The given node provides 0% output capability	S^3	0

$$S^{i,j} = \frac{N_{i,j}}{N} \tag{17}$$

Transmission is the main task of edges and the degradation of edges depends on the decrease of the transmission ability which can be described as the energy transfer state in EFFN.

$$\boldsymbol{S}_{i,j}^{(\mathrm{l})} = [s_{i,j}^{(\mathrm{l})}, \varphi_{i,j}^{(\mathrm{l-in})}(t)] \tag{18}$$

$$S_{i,j}^{(\mathrm{i})} = [s_{i,j}^{(\mathrm{i})}] \tag{19}$$

where $\boldsymbol{S}_{i,j}^{(\mathrm{l})}$ is the state of an edge of flow energy connecting v_i and v_j, and $S_{i,j}^{(\mathrm{i})}$ is the state of an edge of field energy. For a flow edge, if any element of $\boldsymbol{S}_{i,j}^{(\mathrm{l})}$ equals zero, the edge fails, which can be caused by both $s_{i,j}^{(\mathrm{l})} = 0$ which is corresponding to a physical cut-off of cables, pipes or other connections and $\varphi_{i,j}^{(\mathrm{l-in})}(t) = l_{i,j}^{(\mathrm{l})} d_{i,j}^{(\mathrm{l})}(t)$ which is corresponding to a total leakage of a pipe, a very large resistance of wire and a maximum packet loss of an optical fiber. If all elements of $\boldsymbol{S}_{i,j}^{(\mathrm{l})}$ do not equal zero, the edge is normal or at a degradation status. For a field edge, there are only two states: normal and failure, which is decided by $s_{i,j}^{(\mathrm{i})}$.

The propagation begins when a degradation occurs. A node can only be affected by the other nodes which are connected to it by flow edges or field edges. Two nodes v_i and v_j only have three connection types: by a flow edge, by a field edge and both by a flow edge and a field edge.

To analyze the energy transferring and its effect, the network in Fig. 3(b) is taken for an example. It is supposed that, at time t_1, every node in the network is normal and every edge is reliable. At time $t_1 + 1$, a random shock works on node v_3 and causes a failure, and then, $c_3(t_1 + 1) = 0$. Just considering the flow edges, node v_4 stops working because there is no input energy. The output of node v_2 decreases to zero and according to the energy balance in Eq. (2), $\varphi_2^{(\mathrm{out})}(t+1) = 0$ which leads to a decrease of $\eta_2(t+1)$ and more energy dissipation $\psi_2^{(\mathrm{out})}(t_1 + 1)$. The decrease of $\eta_2(t+1)$ leads to a decrease of $c_2(t_1 + 1)$ and changes the state $S_2(t+1)$. At next time unit $t_1 + 2$, because of the decrease of $c_2(t_1 + 2)$, an overload may happen on node v_2, and a continuous degradation process emerges. Considering the field edges, $\psi_2^{(\mathrm{out})}(t_1 + 1)$ affects both v_3 and v_4. v_3 fails and suffers no more degradation, and although v_4 stops working at $t_1 + 1$, the state of v_4 is still normal and may transfer to a degradation state whose probability is influenced by the distance of the two nodes and defined as the influencing intensity $I_{i,j}(T)\big|_{t_1}$.

$$I_{i,j}(T)\big|_{t_1} = \frac{1}{l_{i,j}} \int_{t_1}^{T} a^{t-T} \psi_i^{(\mathrm{out})}(t)\mathrm{d}t \tag{20}$$

Since the field energy will not vanish immediately, a loss coefficient a^{t-T} is multiplied by the energy which is generated at t and acts at T. The influencing intensity $I_{i,j}(T)\big|_{t_1}$ means that, from time t_1 to T, the output field energy of v_i influences v_j cumulatively. $\mathbf{CDCM}_{\mathrm{i,j}}$ is the one-step transferring probability matrix under field intensity $I_{i,j}(T)\big|_{t_1}$, which is known as the Coupling Degradation Coefficient Matrix (CDCM).

$$\mathbf{CDCM}_{i,j}(I_{i,j}(T)\big|_{t_1}) = \begin{bmatrix} b_{i,j}^{0,0} & b_{i,j}^{0,1} & \cdots & b_{i,j}^{0,n} \\ b_{i,j}^{1,0} & b_{i,j}^{1,1} & \cdots & b_{i,j}^{1,n} \\ \vdots & \vdots & \ddots & \vdots \\ b_{i,j}^{m,0} & b_{i,j}^{m,1} & \cdots & b_{i,j}^{m,n} \end{bmatrix} \tag{21}$$

$b_{i,j}^{m,n}$ is the probability that the node v_i with state m will make the node v_j transfer to state n under field intensity $I_{i,j}(T)_{t_1}\Big|$. The propagation stops when $S_i(t+1) = S_i(t), i = 1, 2, ..., n$, and meanwhile, $I_{i,j}(T)\big|_{t_1} < \varepsilon, i = 1, 2, ..., n$ where ε is the threshold at which $b_{i,j}^{m,n} \to 0$.

4. An application to aviation actuation system

The proposed EFFN is universal in modeling complex mechatronic systems. Aviation actuation system influences the performance and safety of an aircraft which are directly related to the life of passengers. As a typical complex mechatronic system, the aviation actuation system can be hardly modeled by traditional networks, especially the degradation propagation process under fluid-thermal-solid coupling interaction.

A simplified part of the actuation system of Airbus 380 is taken as an example, which is shown in Fig. 4. Two dissimilar redundancy actuation systems drive left middle aileron and right middle aileron, respectively. For simplicity, the coordinate system is not shown. Nodes V_2, V_3 and v_4 constitute a Hydraulic Actuation System (HAS) which suffers from fluid-solid coupling effect. Nodes v_5, v_6 and v_7 constitute an electro-hydrostatic actuation system (EHAS) where thermal-vibration coupling effect is one of the main degradation modes. Each component, under different efficiencies, has its own ADR which is not the key item in the proposed system. Therefore, a list of general state transition rates based on mechanical failure rate[2] under high efficiency ($(\eta_{\text{high}} \in [0.5\eta(0), \eta(0)])$) and low efficiency ($(\eta_{\text{low}} \in [0.5\eta(0)])$) shown in Table 2 is used to replace all the autologous degradation rates of different components. The accumulative energy of fluid-solid coupling decays rapidly over time, while that of thermal-vibration declines more slowly. To distinguish the two kinds of field energy, the attenuation rate of energy dissipated by fluid-solid is defined as 0.05 and that by thermal-vibration is 0.8. The influence coefficient between nodes under high-level field energy ($(I_{\text{high}} \in [w, +\infty])$) and low-level field energy ($(I_{\text{low}} \in [0, w])$) of different nodes are listed in Table 3.

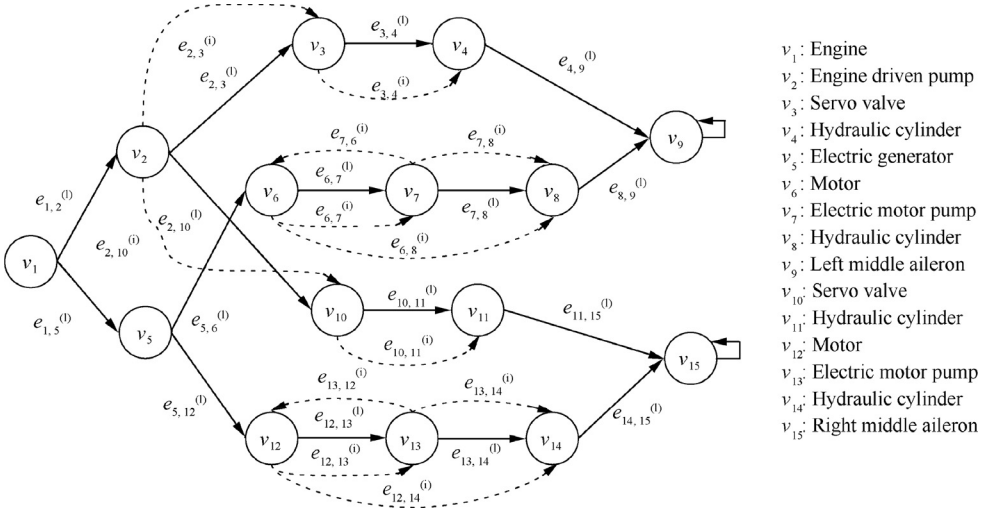

Fig. 4 Part of actuation network on Airbus 380.

Table 2 General state transition rates.

State transition	Probability (High efficiency/ Low efficiency)	State transition	Probability (High efficiency/ Low efficiency)
$S^{0,0}$	0.9999978/0.98	$S^{2,0}$	0/0
$S^{0,1}$	0.0000022/0.01	$S^{2,1}$	0/0
$S^{0,2}$	0 /0.01	$S^{2,2}$	0.99/0.95
$S^{0,3}$	0/0	$S^{2,3}$	0.01/0.05
$S^{1,0}$	0/0	$S^{3,0}$	0/0
$S^{1,1}$	0.9991/0.97	$S^{3,1}$	0/0
$S^{1,2}$	0.0009/0.02	$S^{3,2}$	0/0
$S^{1,3}$	0 /0.01	$S^{3,3}$	1/1

Table 3 Influence coefficient of different nodes.

CDCM	Coefficient matrix	CDCM	Coefficient matrix
$\mathbf{CDCM}_{2,3}(I_{low})$ $\mathbf{CDCM}_{2,10}(I_{low})$	$\begin{bmatrix}0.999946 & 0.999901 & 0.99 & 0.9\\ 0.000054 & 0.000098 & 0.007 & 0.05\\ 0 & 0.000001 & 0.002 & 0.046\\ 0 & 0 & 0.001 & 0.004\end{bmatrix}$	$\mathbf{CDCM}_{6,8}(I_{low})$ $\mathbf{CDCM}_{12,14}(I_{low})$	$\begin{bmatrix}0.99991 & 0.9995 & 0.9991 & 0.9987\\ 0.00006 & 0.0003 & 0.0006 & 0.0006\\ 0.00003 & 0.0001 & 0.0002 & 0.0004\\ 0 & 0.0001 & 0.0001 & 0.0003\end{bmatrix}$
$\mathbf{CDCM}_{2,3}(I_{high})$ $\mathbf{CDCM}_{2,10}(I_{high})$	$\begin{bmatrix}0.9 & 0.7 & 0.6 & 0.4\\ 0.1 & 0.1 & 0.2 & 0.3\\ 0 & 0.1 & 0.1 & 0.2\\ 0 & 0.1 & 0.1 & 0.1\end{bmatrix}$	$\mathbf{CDCM}_{6,8}(I_{high})$ $\mathbf{CDCM}_{12,14}(I_{high})$	$\begin{bmatrix}0.9 & 0.8 & 0.8 & 0.7\\ 0.1 & 0.1 & 0.01 & 0.1\\ 0 & 0.1 & 0.05 & 0.1\\ 0 & 0 & 0.05 & 0.1\end{bmatrix}$
$\mathbf{CDCM}_{3,4}(I_{low})$ $\mathbf{CDCM}_{10,11}(I_{low})$	$\begin{bmatrix}0.999978 & 0.999932 & 0.99987 & 0.997\\ 0.000022 & 0.000048 & 0.0001 & 0.002\\ 0 & 0.00002 & 0.00002 & 0.0009\\ 0 & 0 & 0.00001 & 0.0001\end{bmatrix}$	$\mathbf{CDCM}_{7,6}(I_{low})$ $\mathbf{CDCM}_{13,12}(I_{low})$	$\begin{bmatrix}0.9936 & 0.9914 & 0.985 & 0.96\\ 0.005 & 0.0067 & 0.009 & 0.02\\ 0.001 & 0.0011 & 0.004 & 0.012\\ 0.0004 & 0.0008 & 0.002 & 0.008\end{bmatrix}$
$\mathbf{CDCM}_{3,4}(I_{high})$ $\mathbf{CDCM}_{10,11}(I_{high})$	$\begin{bmatrix}0.9 & 0.7 & 0.3 & 0.1\\ 0.1 & 0.2 & 0.3 & 0.1\\ 0 & 0.1 & 0.2 & 0.3\\ 0 & 0 & 0.2 & 0.5\end{bmatrix}$	$\mathbf{CDCM}_{7,6}(I_{high})$ $\mathbf{CDCM}_{13,12}(I_{high})$	$\begin{bmatrix}0.9 & 0.7 & 0.3 & 0.1\\ 0.1 & 0.3 & 0.3 & 0.3\\ 0 & 0 & 0.2 & 0.2\\ 0 & 0 & 0.2 & 0.4\end{bmatrix}$
$\mathbf{CDCM}_{6,7}(I_{low})$ $\mathbf{CDCM}_{12,13}(I_{low})$	$\begin{bmatrix}0.9991 & 0.98 & 0.94 & 0.9\\ 0.0006 & 0.014 & 0.041 & 0.06\\ 0.0003 & 0.004 & 0.013 & 0.028\\ 0 & 0.002 & 0.006 & 0.012\end{bmatrix}$	$\mathbf{CDCM}_{7,8}(I_{low})$ $\mathbf{CDCM}_{13,14}(I_{low})$	$\begin{bmatrix}0.99993 & 0.9995 & 0.9994 & 0.9989\\ 0.00007 & 0.0005 & 0.0003 & 0.0004\\ 0 & 0 & 0.0002 & 0.0004\\ 0 & 0 & 0.0001 & 0.0003\end{bmatrix}$
$\mathbf{CDCM}_{6,7}(I_{high})$ $\mathbf{CDCM}_{12,13}(I_{high})$	$\begin{bmatrix}0.9 & 0.6 & 0.1 & 0.1\\ 0.1 & 0.2 & 0.5 & 0.2\\ 0 & 0.1 & 0.2 & 0.4\\ 0 & 0.1 & 0.2 & 0.3\end{bmatrix}$	$\mathbf{CDCM}_{7,8}(I_{high})$ $\mathbf{CDCM}_{13,14}(I_{high})$	$\begin{bmatrix}0.9 & 0.8 & 0.8 & 0.7\\ 0.1 & 0.1 & 0.01 & 0.1\\ 0 & 0.1 & 0.05 & 0.1\\ 0 & 0 & 0.05 & 0.1\end{bmatrix}$

Table 4 Equivalent average energy demand of a controlled surface.

No.	Flight stage	Energy demand	During time
1	Taxiing Departure	26.5	12.8
2	Takeoff	60.6	0.91
3	Climb	60.6	21.9
4	Cruise	7.6	132.1
5	Descend	41.6	24.6
6	Approach	18.9	1.79
7	Taxiing Landing	83.3	8.7
8	Emergency	123	0.30

For real aircraft, the energy is not transferred stochastically in the network. The nodes are controlled by flight plan, which means that the energy demands are determined by the terminal users[29]. An equivalent average energy demand of a controlled surface in each flight phase is shown in Table 4.

Table 6 Node data of Fig. 4.

Node	$c(0)$	w	$\eta(0)$	Node	$c(0)$	w	$\eta(0)$
v_2 *	259	24	0.98	v_9	180	36	0.99
v_3	230	10	0.7	v_{10}	245	13	0.7
v_4	222	30	0.9	v_{11}	215	26	0.9
v_5	350	50	0.99	v_{12}	286	42	0.9
v_6	283	44	0.9	v_{13}	229	15	0.98
v_7	232	17	0.98	v_{14}	232	19	0.9
v_8	219	21	0.9	v_{15}	183	32	0.99

* v_1 is the source node.

Commonly, there is no physical isolation change during the system running, so the field edges are believed to be reliable. To simplify the problem, the dimensionless dissipation rate of each flow edge is set to be 0.1 and the corresponding lengths

Table 5 Edge data of Fig.4.

Edge	Length	Edge	Length	Edge	Length	Edge	Length
$e^{(l)}_{1,2}$	2	$e^{(l)}_{5,12}$	100	$e^{(l)}_{13,14}$	0.1	$e^{(i)}_{7,6}$	0.1
$e^{(l)}_{1,5}$	2	$e^{(l)}_{6,7}$	0.1	$e^{(l)}_{14,15}$	0.5	$e^{(i)}_{7,8}$	0.1
$e^{(l)}_{2,3}$	4	$e^{(l)}_{7,8}$	0.1	$e^{(i)}_{2,3}$	2	$e^{(i)}_{10,11}$	1
$e^{(l)}_{2,10}$	150	$e^{(l)}_{8,9}$	0.5	$e^{(i)}_{2,10}$	54	$e^{(i)}_{12,13}$	0.1
$e^{(l)}_{3,4}$	1	$e^{(l)}_{10,11}$	1	$e^{(i)}_{3,4}$	0.5	$e^{(i)}_{12,14}$	0.1
$e^{(l)}_{4,9}$	0.5	$e^{(l)}_{11,15}$	0.5	$e^{(i)}_{6,7}$	0.1	$e^{(i)}_{13,12}$	0.1
$e^{(l)}_{5,6}$	5	$e^{(l)}_{12,13}$	0.1	$e^{(i)}_{6,8}$	0.1	$e^{(i)}_{13,14}$	0.1

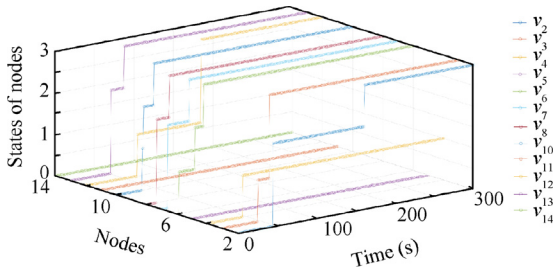

Fig. 5 Degradation states of nodes.

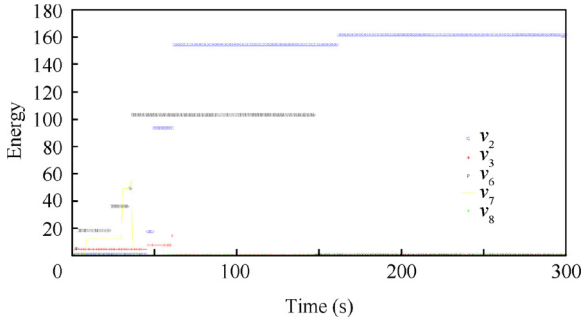

Fig. 6 Field output energy of nodes.

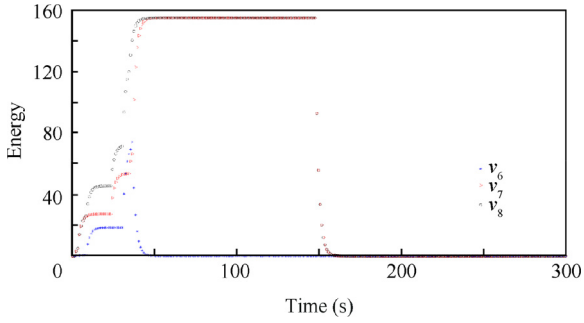

Fig. 7 Field input energy of nodes.

of flow edges and field edges are shown in Table 5. By supposing that the same kind of nodes have individual differences, the node data are shown in Table 6.

In order to demonstrate the propagation scenario instead of an actual life-cycle degradation of the system, the transition probabilities shown in Table 3 are given much higher values in the simulation than the real situation so that the propagation will not last too long and the capacities of nodes are close to the emergency stage so that the nodes are inherently vulnerable. Assume that each node works under rated condition in the beginning, and at the emergency stage, the motor of EHAS at left middle aileron degrades to the slight fault state firstly. Fig. 5 shows the results from a single simulation. We can see that the transition of degradation states of each node presents the degradation propagation path: the motor of EHAS at left middle aileron v_6 degrades, afterwards the pump v_7 connected to it degrades and then the cylinder v_8 transfers to a severe fault state. The other nodes degrade as shown in the figure, and the figure is one single simulation result that some of the nodes do not degrade by the effect of flow and field, which degrades by its autologous degradation instead of the propagation from other nodes. The node then becomes another starting point of degradation propagation.

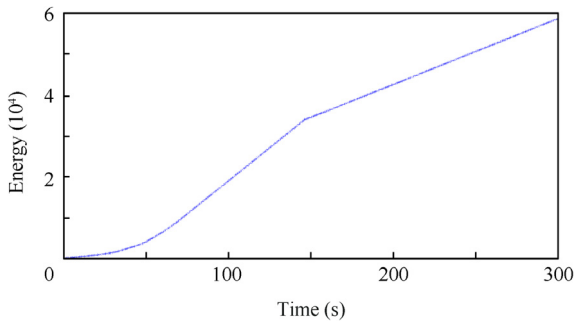

Fig. 8 Total dissipation energy.

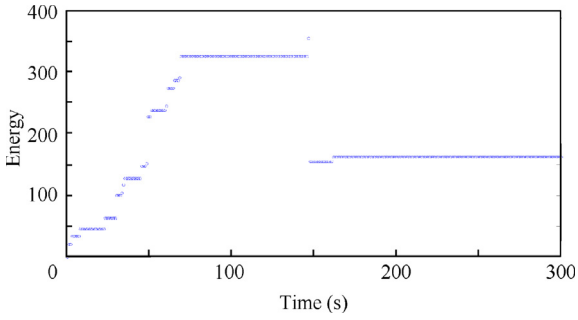

Fig. 9 Dissipation energy of each step.

Both flow and field energy may cause the degradation. Fig. 6 shows the field output energy of the actuation system on the left middle aileron, which helps to analyze the degradation reasons. At the second time step, an overload is applied on node v_6. The motor v_6 transfers to the slight fault state at the fourth time step, which leads to a slight overload on the motor and more energy dissipation to the field. There is no increase in field output energy of node v_7 which connects to v_6 by field edge and no state change of nodes v_5 and v_7 which connect to v_6 by flow edges. Thus, the degradation of v_6 at the fourth time step to a severe fault state is caused by the overload on itself. The second degradation of the system happens on node at the seventh time step at the seventh time step. The output field energy of v_6 is 18.0889 when node v_7 degrades, and from Fig. 7, we can see that, after several time steps, the accumulative input energy on v_7 by field reaches 17. The influencing intensity of energy by v_6 is higher than w_7 and a high level influence coefficient $\mathbf{CDCM}_{6,7}(I_{\text{high}})$ shown in Table 3 is applied. Because v_7 is at normal state before state transferring, according to Table 2, the autologous degradation probability from normal to severe fault is zero. Then we can confirm that the degradation is caused by v_6. Otherwise, the autologous degradation possibility may also be considered.

The total dissipation energy by field is shown in Fig. 8. The slope of the energy curve is small at first, which means that less overloads happen and most nodes of the system are at normal states. While the degradation occurs, the slope becomes larger and larger, which can also be seen in Fig. 9. We can find that, from time step 70, the slope remains a constant until time step 160. Compared to Fig. 5, most nodes already fail before time step 70, which means that most nodes stop working and the

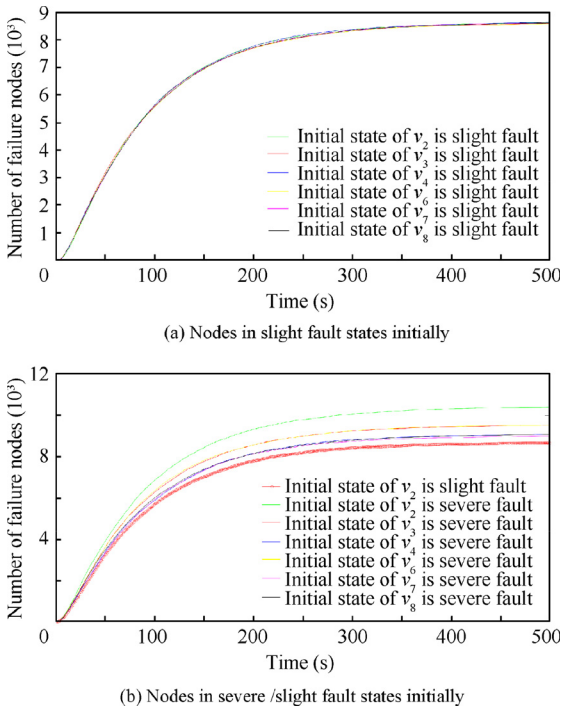

Fig. 10 Dynamic failure process of system with dependent components.

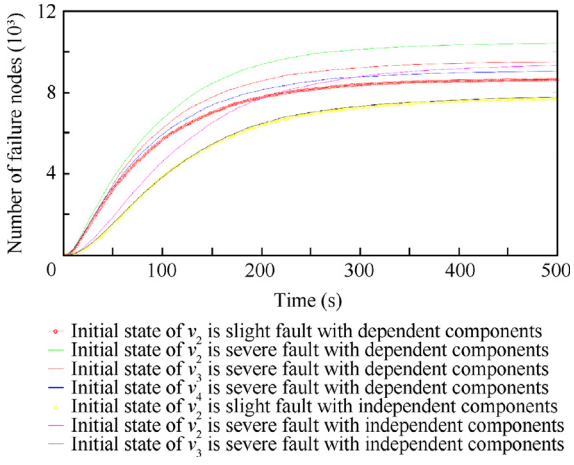

Fig. 11 Dynamic failure process of system.

field energy is generated by minor nodes v_2 and v_5. Node v_2 finally fails because of long time overload and gives rise to a dramatic decrease on the slope. The slope then remains a constant until the simulation stops.

Since the degradation of components is modeled as a stochastic state transition process, the inherent uncertain should be considered. A Monte-Carlo simulation is conducted on the actuation system and the statistical results are obtained. By setting different initial degradation states, the dynamic failure process of the system is shown in Fig. 10. Each result is the accumulation of 1000 realizations. Fig. 10(a) shows the results when the initial degradation state of each node is slight fault, from which we can see that, in such situation, the failure processes triggered by different slight faults are with little difference. When the initial degradation state of each node is

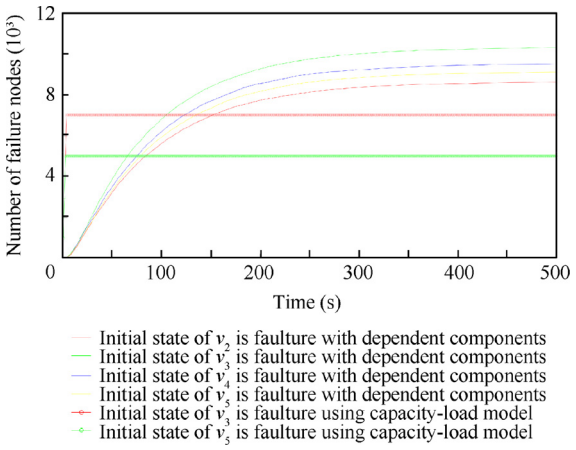

Fig. 12 Comparison of capacity-load model and EFFN.

severe fault, more difference can be found, that is, the system statistically arrives at a more severe failure state, which can be explained by the difference of state transition rate under low efficiency and high efficiency. Node v_2 affects the system most, which is consistent with the given scenario. Meanwhile, node v_3 and node v_6 cause more impacts than node v_4 , node v_7 and node v_8 because of the load dynamics and topology.

By setting all the elements in CDCM to be ones, the system is transferred to a system with independent components, which means that the degradation of the system is determined by the dynamic loads completely. The dynamic loads affect the system with independent components by ADR. With higher loads or lower efficiency, the independent components are more likely to degrade. The comparative results are shown in Fig. 11 By neglecting the influence of dependency among components, the number of failure nodes decreases sharply compared with the dependent components. Meanwhile, the difference between the influence of initial severe states and initial slight states becomes larger. The initial severe state of node v_2 has a greater impact on the system.

To make a comparison with the traditional methods, we consider a static model using capacity-load analysis which is a commonly used method to analyze the cascading failures. The capacity-load model[30] considered that the capacity of network node is constrained by cost, and assumed a linear relationship between the capacity and load of nodes. Combined with the concept of capacity-load model, the capacity of each node is defined the same as EFFN, which is listed in Table 6. Cascades are assumed to be triggered by the removal of single nodes. The comparative results are shown in Fig. 12. From the figure, we can see that since the capacity-load model is a static model which cannot reflect the degradation process of each component, the number of failure nodes reaches the steady state within a very short time. The result of capacity-load model actually does not concern the uncertainty caused by the degradation process, nor the interaction between nodes which share the same environment, which leads to a lower steady value than using EFFN method.

5. Conclusions

For a complex mechatronic system, the effect of a fault node may start from degradation instead of failure. The degradation

may spread along traditional edges like cables, roads, radio wave, pipes and so on. Meanwhile, other systems or environment may have an effect on the given system. Those influences of other systems or environment which cannot be described by traditional networks but actually play an important role in the spreading process are modeled as field energy in the proposed novel EFFN. If there is only one sink node and there is no field energy, the network can be regarded as a stochastic flow network. To give a general expression of flow effects and field effects, the proposed EFFN utilizes the concept of energy that different kinds of flow and field effects are uniformly modeled by flow energy and field energy. Compared with the traditional networks, the flow energy is used to replace the flow while the field energy is used to present the effect of the environment and other systems. The field energy can conduct accumulative or shock impact on the connected nodes by assigning different attenuation coefficients, for example, the temperature changes slowly over time and vibration decays heavily. Considering the degradation of the node itself, ADR is used to describe the state transition. The correlations between different nodes with different degradation states are modeled as CDCM. The strength of a field energy on a node is measured by time-dependent influencing intensity in this work.

The proposed method is applied to a multi-field coupling degradation propagation process in an aviation actuation system. The propagation path is shown in a time-dependent state transition figure which provides the order of degradation intuitively. By combining the output field energy and the input field energy, the degradation modes are analyzed. For a measurable energy system, the application provides a method to estimate the possible failure reason by system energy atlas. The analyzed result is consistent with the given scenario. Compared with the traditional methods, the proposed method takes advantages in analyzing the joint effect of load dynamics and components dependency by providing dynamic failure process, and meanwhile, establishes a unified description of the interdependency between flow energy and field energy.

Acknowledgments

This study was co-supported by the National Natural Science Foundation of China (Nos. 51875014, 51575019, 51620105010), Natural Science Foundation of Beijing Municipality (No. L171003) and Program 111 of China.

References

1. Feng D, Lin S, Yang Q, et al. Reliability evaluation for traction power supply system of high-speed railway considering relay protection. *IEEE Trans Transp Electrif* 2018;**5**(1):285–98.
2. Wang S, Cui X, Shi J, et al. Modeling of reliability and performance assessment of a dissimilar redundancy actuation system with failure monitoring. *Chin J Aeronaut* 2016;**29**(3):799–813.
3. Guo H, Yu SS, Iu HH, et al. A complex network theory analytical approach to power system cascading failure—from a cyber-physical perspective. *Chaos: Int J Nonlinear Sci* 2019;**29**(5):053111.
4. Schäfer B, Witthaut D, Timme M, et al. Dynamically induced cascading failures in power grids. *Nat Commun* 2018;**9**(1):1975.
5. Zhou J, Huang N, Coit DW, et al. Combined effects of load dynamics and dependence clusters on cascading failures in network systems. *Reliab Eng Syst Saf* 2018;**170**:116–26.
6. Enrico Z, Mengfei F, Zhiguo Z, et al. Application of reliability technologies in civil aviation: lessons learnt and perspectives. *Chin J Aeronaut* 2019;**32**(1):143–58.
7. Watts DJ, Strogatz SH. Collective dynamics of "small-world" networks. *Nature* 1998;**393**:440–2.
8. Gao J, Li G, Gao Z. Fault propagation analysis for complex system based on small-world network model. *Reliab Maintain Symp* 2008;359–64.
9. Barabási A, Albert R. Emergence of scaling in random networks. *Science* 1999;286.
10. Ren HP, Song J, Yang R, et al. Cascade failure analysis of power grid using new load distribution law and node removal rule. *Phys A* 2016;**442**(1):239–51.
11. Wei X, Gao S, Huang T, et al. Complex network-based cascading faults graph for the analysis of transmission network vulnerability. *IEEE Trans Ind Inf* 2018;**15**(3):1265–76.
12. Jing K, Tang L. Robustness of complex networks: cascading failure mechanism by considering the characteristics of time delay and recovery strategy. *Statist Mech Appl Phys A* 2019;122061.
13. Lin S, Wang Y, Jia L, et al. Reliability assessment of complex electromechanical systems: a network perspective. *Qual Reliab Eng Int* 2018;**34**(11):772–90.
14. Lin S, Wang Y, Jia L. System reliability assessment based on failure propagation processes. *Complexity* 2018;**2018**(3):1–19.
15. Zhang DX, Zhao D, Guan ZH, et al. Probabilistic analysis of cascade failure dynamics in complex network. *Phys A* 2016;**461**:299–309.
16. Zhang Y, Yağan O. Optimizing the robustness of electrical power systems against cascading failures. *Sci Rep* 2016;**6**:27625.
17. Li T, Wang S, Shi J, et al. An adaptive-order particle filter for remaining useful life prediction of aviation piston pumps. *Chin J Aeronaut* 2018;**31**(5):941–8.
18. Li T, Shi J, Wang S, et al. Mesoscale numerical modeling for predicting wear debris generation. *Tribol Lett* 2019;**67**(2):38.
19. Liu RR, Li M, Jia C-X. Cascading failures in coupled networks: the critical role of node-coupling strength across networks. *Sci Rep* 2016;**6**:35352.
20. Su X, Ma J, Chen N, et al. Cascading failures on interdependent networks with multiple dependency links and cliques. *Phys A* 2019;**526** 120907.
21. Zhong J, Zhang F, Yang S, et al. Restoration of interdependent network against cascading overload failure. *Phys A* 2019;**514**:884–91.
22. Liu R-R, Li M, Jia C-X, et al. Cascading failures in coupled networks with both inner-dependency and inter-dependency links. *Sci Rep* 2016;**6**:25294.
23. Helmut S. *Failure mode and effectanalysis: FMEA from theory to execution;* Milwaukee, Wisconsin: ASQ Press; 2003.
24. Gao H, Fei C, Bai G, et al. Reliability-based low-cycle fatigue damage analysis for turbine blade with thermo-structural interaction. *Aerosp Sci Technol* 2016;**49**:289–300.
25. Lin YK. A simple algorithm for reliability evaluation of a stochastic-flow network with node failure. *Comput Oper Res* 2001;**28**(13):1277–85.
26. Lin YK. Reliability of a stochastic-flow network with unreliable branches & nodes, under budget constraints. *IEEE Trans Reliab* 2004;**53**(3):381–7.

27. Lin YK. Network Reliability of a Time-based multistate network under spare routing with p minimal paths. *IEEE Trans Reliab* 2011;**60**(1):61–9.
28. Lin YK, Chang PC. Evaluation of system reliabilities for a maintainable stochastic-flow network. *IEEE Trans Reliab* 2012;**61**(2):398–409.
29. Ma Z, Wang S, Zhang C, et al. A load sequence design method for hydraulic piston pump based on time-related Markov matrix. *IEEE Trans Reliab* 2018;**99**:1–12.
30. Motter AE, Lai Y-C. Cascade-based attacks on complex networks. *Phys Rev E* 2002;**66**(6): 065102.